Supporting Information of

A Hybrid Nanozymes in situ Oxygen Supply Synergistic Photothermal-/Chemotherapy of Cancer Management

Xufeng Zhu[a,b,1], Xu chen[a,b,1], Dongliang Huo[a,b], Jieqiong Ceng[a,b], Zhi Jia[a,b], Yanan Liu[a,*], Jie Liu[a,b,*]

a.Shenzhen Longhua Maternity and Child Healthcare Hospital, Shenzhen, 518110, China.

b.Department of Chemistry, College of Chemistry and Materials Science, Jinan University, Guangzhou 511436, People's Republic of China.

E-mail: yananliu0321@163.com; tliuliu@jnu.edu.cn.

*Corresponding author.

1These authors contributed equally to the work.

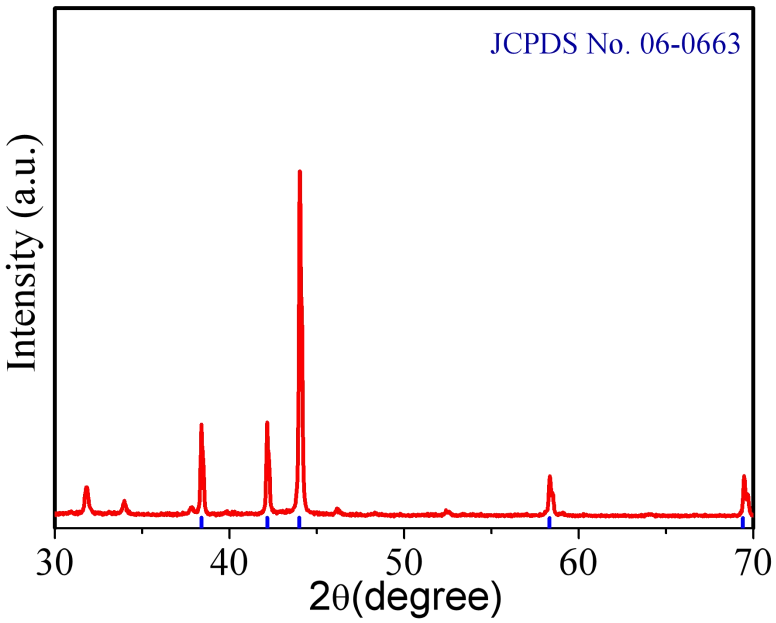

Figure S1. XRD results of Ru NPs.

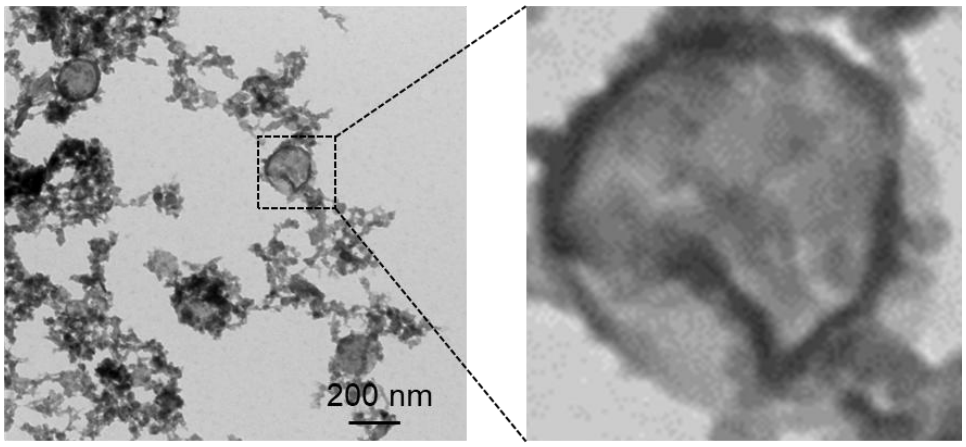

Figure S2. TEM micrograph of erythrocyte membrane vesicles. RBCm has a particle size of approximately 200 nm.

Magnified image shows that RBCm has a good saclike appearance [1, 2].

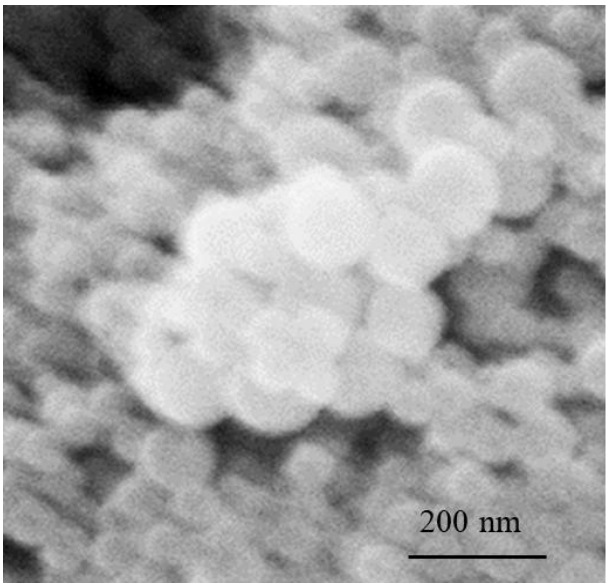

Figure S3. SEM micrograph of RBCm@Ru@MnO_2, it has good spherical morphology and dispersion.

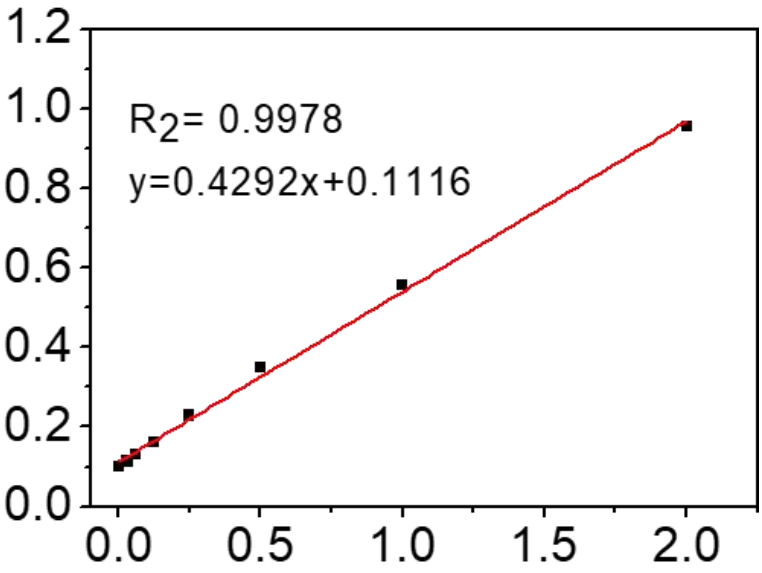

Figure S4. BCA kit test protein of RBCm@Ru@MnO_2, the surface protein loading rate of RBCm@Ru@MnO_2 was determined by the BCA kit to be about 53.28% [3].

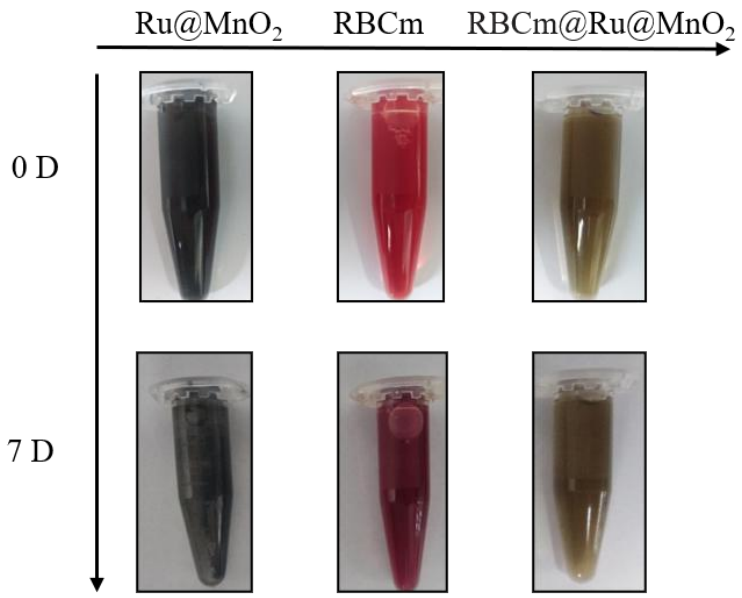

Figure S5. The particle size changes of $Ru@MnO_2$ and $RBCm@Ru@MnO_2$ after being placed in cell culture medium (pH 7.4) for 7 days. Compared with $Ru@MnO_2$, $RBCm@Ru@MnO_2$ still has good dispersion, it is indicated that the coating of the erythrocyte membrane can give $Ru@MnO_2$ a good physiological activity.

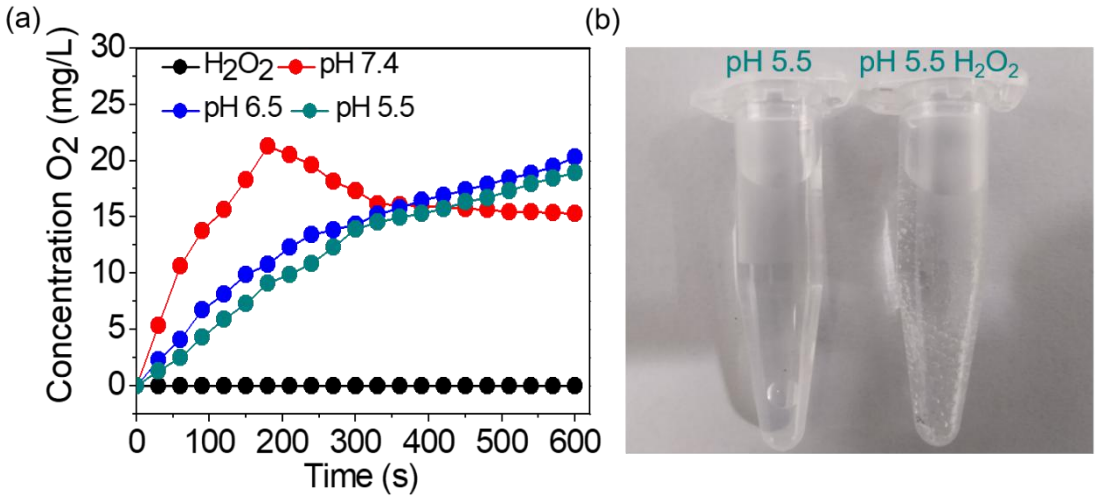

Figure S6. Pictures of RBCm@Ru-MnO_2@DOX dispersed in dispersed in pH 5.5 solutions with or without H_2O_2. Produces a large amount of O_2 to alleviate the hypoxia of solid tumors and indirectly prevent tumor cell regeneration

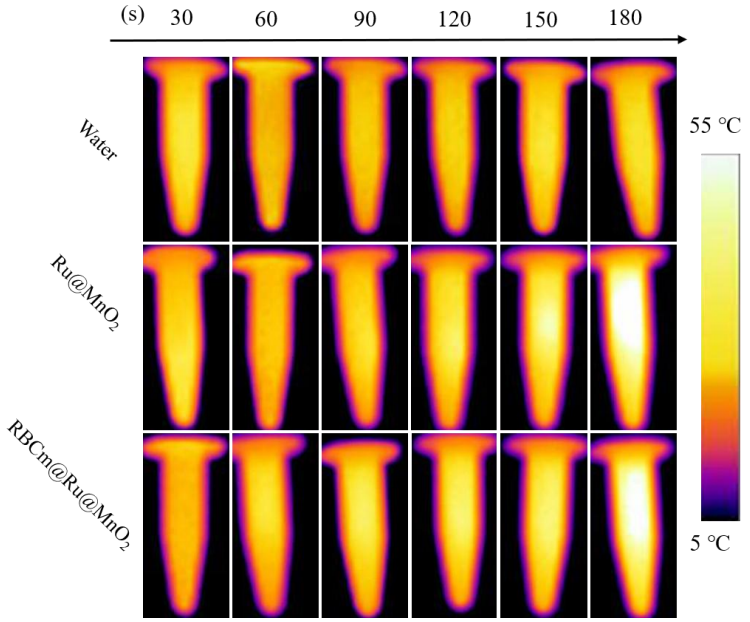

Figure S7. Infrared thermal images of Water, Ru@MnO_2 and RBCm@Ru@MnO_2.

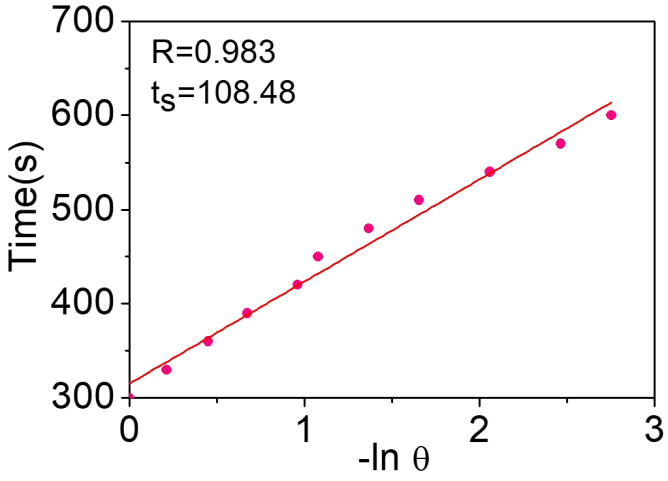

Figure S8. Linear time data *versus*-lnθ obtained from the cooling period. RBCm@Ru-MnO_2 exhibited high photothermal conversion efficiency (36.99%).

The photothermal conversion efficiency (η) of RBCm@Ru-MnO_2can be calculated as following equations:

$$\eta = [hs(T_{max}-T_{surr})-Q_{dis}]/[I(1-10^{-A808})]*100\%$$

Where η is the photothermal conversion efficiency (×100%), T_{max} is the highest temperature of the sample, T_{surr} is the

ambient temperature (unit: °C), I is the laser power used, A808 is the absorbance value (dimensionless) of the sample at the excitation wavelength, Qdis is the change in heat when the reagent is blank, h is the thermal conversion efficiency of the system and S is the surface area of the vessel.The value of Q_{dis} can be determined separately from the reagent blank.

$$hs = (m * C_{H2O})/T_s$$

Where m is the mass of the solution (unit: g), C_{H2O} is the specific heat capacity of water (4.2 J × g^{-1} × $°C^{-1}$), Ts is the time constant of the system (dimensionless).The value of Ts can be calculated by equation (3):

$$t = -Ts \ln(\Theta) = -Ts \ln(T-T_{surr})/(T_{max}-T_{surr})$$

Where t is the time during cooling (unit: s), Θ is the thermal drive constant, T is the instantaneous temperature at t time, Tmax is the highest temperature of the sample. Tsurr is the ambient temperature, thus the Ts value can be obtained by linearly fitting the negative value of the cooling time to the natural logarithm of the thermal drive constant [4].

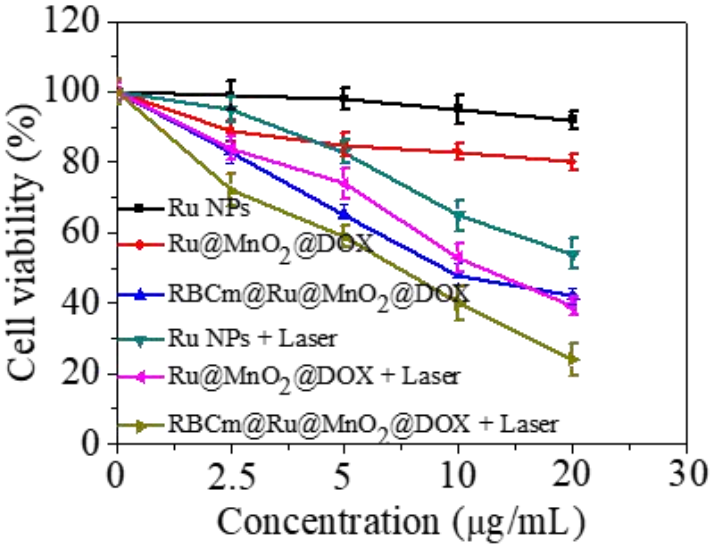

Figure S9. MTT of RBCm@Ru@MnO_2@DOX with or without Laser. Chemotherapy/photothermal therapy significantly inhibits the activity of tumor cells.

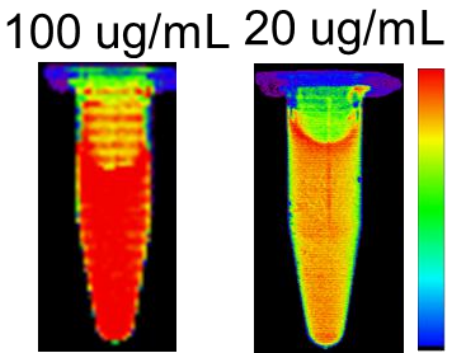

Figure S10. Degree of fluorescence on RBCm@Ru@MnO_2@DOX, the fluorescence density of RBCm@Ru@MnO_2@DOX appears to be positively correlated with the concentration of RBCm@Ru@MnO_2@DOX.

Indicates the possibility that it can be used for in vivo tracking.

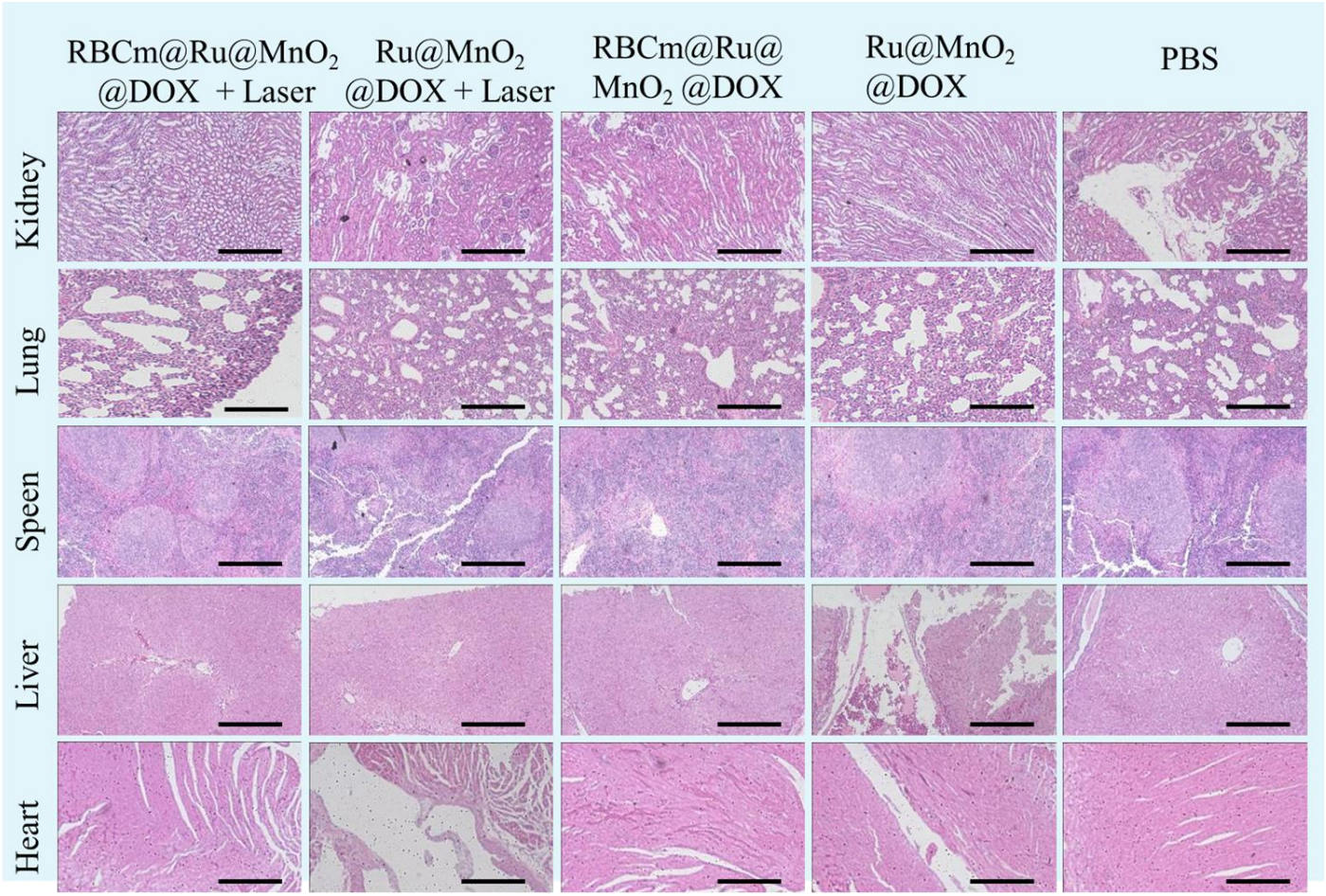

Figure S11. Histological analyses of the major tissues after therapy with Ru@MnO_2@DOX, RBCm@Ru@MnO_2@DOX with Laser (1W/cm^2) or without Laser. The results indicate good safety for normal tissues at given drug concentration. Scale bar:100 m.

References

[1] Chen, W.; Zeng, K.; Liu, H.; Ouyang, J.; Wang, L.; Liu, Y.; Wang, H.; Deng, L.; and Liu, Y. Cell Membrane Camouflaged Hollow Prussian Blue Nanoparticles for Synergistic Photothermal-/Chemotherapy of Cancer. *Adv. Funct. Mater.* ***2017****, 1605795.*

[2] Zhang, L.; Wang, Z.; Zhang, Y.; Cao, F.; Dong, K.; Ren, J.; and Qu, X.; Erythrocyte Membrane Cloaked Metal-Organic Framework Nanoparticle as Biomimetic Nanoreactor for Starvation-Activated Colon Cancer Therapy. *ACS Nano.* ***2018****, 12, 10201−10211.*

[3] FRED V. PLAPP, MARK M. KOWALSKI, LOWELL TILZER, PEGGY J. BROWN, JAMES EVANS, AND MASAHIRO CHIGA. Partial purification of Rho (D) antigen from Rh positive and negative erythrocytes. *Proceedings of the National Academy of Sciences.****1979****,76, 2964–2968.*

[4] Xiao, Z.; Xu, C.; Jiang, X.; Zhang, W.; Peng, Y.; Zou, R.; Huang, X.; Liu, Q.; Qin, Z.; and Hu, J. Hydrophilic bismuth sulfur nanoflower superstructures with an improved photothermal efficiency for ablation of cancer cells. *Nano Research.* **2016**, 9, 1934-1947.